Shock Waves (1995) 5:127–138

Shock Waves

Experimental investigation on tunnel sonic boom

K. Takayama[1], A. Sasoh[1], O. Onodera[1], R. Kaneko[2], Y. Matsui[2]

[1] Shock Wave Research Center, Institute of Fluid Science, Tohoku University, 2-1-1 Katahira, Aoba-ku, Sendai 980, Japan
[2] East Japan Railway Co., Tokyo Kotsu Kaikan 7th Floor, 2-10-1 Yuraku-cho, Chiyoda-ku, Tokyo 100, Japan

Received August 1, 1994 / Accepted February 15, 1995

Abstract. Upon the entrance of a high-speed train into a relatively long train tunnel, compression waves are generated in front of the train. These compression waves subsequently coalesce into a weak shock wave so that a unpleasant sonic boom is emitted from the tunnel exit. In order to investigate the generation of the weak shock wave in train tunnels and the emission of the resulting sonic boom from the train tunnel exit and to search for methods for the reduction of these sonic booms, a 1 : 300 scaled train tunnel simulator was constructed and simulation experiments were carried out using this facility.

In the train tunnel simulator, an 18 mm dia. and 200 mm long plastic piston moves along a 40 mm dia. and 25 m long test section with speed ranging from 60 to 100 m/s. The tunnel simulator was tilted 8° to the floor so that the attenuation of the piston speed was not more than 10 % of its entrance speed. Pressure measurements along the tunnel simulator and holographic interferometric optical flow visualization of weak shock waves in the tunnel simulator clearly showed that compression waves, with propagation, coalesced into a weak shock wave. Although, for reduction of the sonic boom in prototype train tunnels, the installation of a hood at the entrance of the tunnels was known to be useful for their suppression, this effect was confirmed in the present experiment and found to be effective particularly for low piston speeds. The installation of a partially perforated wall at the exit of the tunnel simulator was found to smear pressure gradients at the shock. This effect is significant for higher piston speeds. Throughout the series of train tunnel simulator experiments, the combination of both the entrance hood and the perforated wall significantly reduces shock overpressures for piston speeds of u_p ranging from 60 to 100 m/s. These experimental findings were then applied to a real train tunnel and good agreement was obtained between the tunnel simulator result and the real tunnel measurements.

Key words: Impulsive pressure wave, Piston problem, Perforated wall, Railway tunnel, Shock wave generation, Sonic boom

Correspondence to: K. Takayama

1. Introduction

The high speed train network in Japan (Shinkansen) has been operated successfully for the past three decades. The cost of the Shinkansen is reported to be comparable approximately to that of the Apollo project in the United States (Lukasiewicz 1976). The success of this train transportation may be closely related to the size of countries and also the population distribution of countries. Japan is, however, a mountainous country so that, in order to have relatively straight railway tracks, many short and long train tunnels have been constructed. When, recently, the train speed was increased from 220 km/h to 270 km/h, it was realized that the high speed train entrance into long train tunnels created sonic booms, which were so loud as to prevent in the near future the possibility of a further increase of the train speed exceeding 300 km/h.

Sonic booms created by high speed train entrance into long tunnels may remind gasdynamicists of a type of piston problem with which they are familiar. That is when a piston which does not completely fill a tube cross section but has a significant clearance between the piston and the tube wall moves along the tube. Then compression waves are generated ahead of it and these coalesce, with propagation, into a shock wave. Hence, it is an interesting research topic to see experimentally and numerically how compression waves driven by a leaky piston in the tunnel simulator coalesce into a shock wave.

Shock waves emitted from train tunnels become booms in the neighborhood of the exits of Shinkansen tunnels. These booms are somewhat analogous to those caused by supersonic flights so that may be called *tunnel sonic booms*. The overpressure of the tunnel sonic boom increases with increase of the train speed. Increase of the train speed will therefore be practically limited until a way of preventing the tunnel sonic boom is achieved. Careful gasdynamic studies are, therefore, urgently needed with the aim of suppressing the train tunnel sonic boom. Sajben (1971) analyzed the wave generation in a train-tunnel system based using an acoustic theory. His analytical result is applicable to relatively low train speeds under 50 m/s (180 km/h). Related research was conducted by the Railway Technical Research Institute of the Japan National Railways (Ozawa et al. 1976; Ozawa 1979). The train speeds under study in those days were at most 55 m/s (200 km/h). The

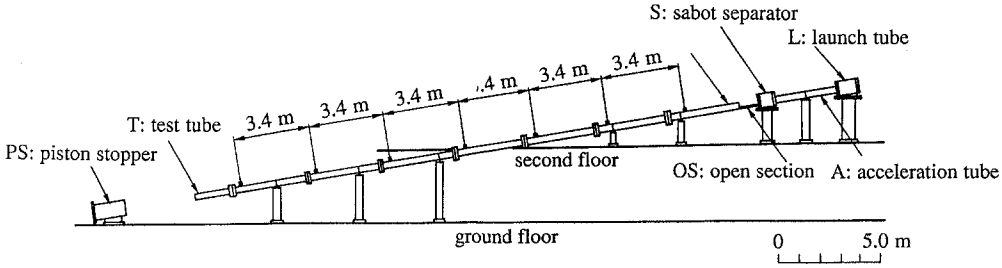

Fig. 1. Scaled train tunnel simulator

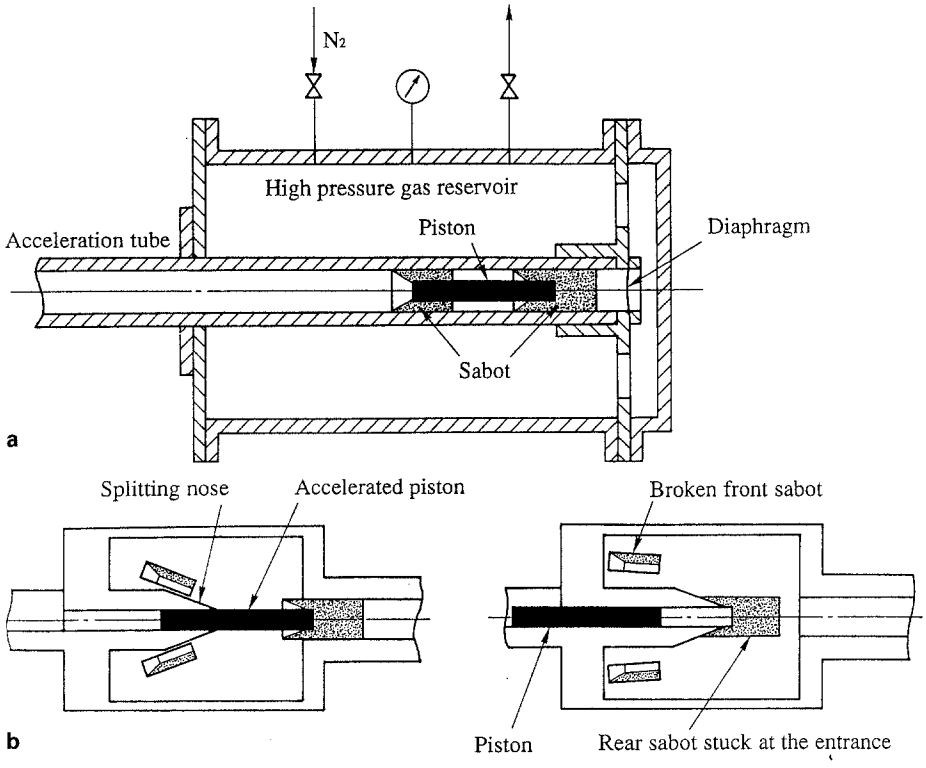

Fig. 2a,b. Driver gas reservoir and sabot separator: **a** high pressure gas reservoir; and **b** sabot separator

pressure profile of the compression waves generated ahead of the train was successfully measured. Compression waves were found to have a finite pressure gradient and the strength of impulsive sound waves released from the tunnel exit was analyzed by the method of characteristics. Based on the acoustic theory, Ozawa et al. (1976) and Ozawa (1979) found that a hood whose shape was short and straight and had an increasing area section, installed at the entrance of the train tunnel was very effective in the reduction of the impulsive sound waves.

Matsuo and Aoki (1992) investigated tunnel sonic booms as unsteady gasdynamic problems and reproduced experimentally, using a shock tube, impulsive pressure waves. Also using TVD finite difference scheme, the formation and propagation of impulsive pressure waves were numerically analyzed (Aoki et al. 1992; Takayama et al. 1993). Peak overpressures of the impulsive pressure waves were scaled with the time derivative of the overpressures at the tube exit (Rudinger 1957; Blake 1986; Matso and Aoki 1992). This relation is applicable to most of the existing Shinkansens as long as the pressure gradient of the compression waves remains finite.

An experimental study was carried out the reduction of train tunnel sonic booms (Takayama et al. 1993; Sasoh et al. 1994a). A 1 : 300 scaled tunnel simulator was constructed and simulation experiments were conducted with it. Simulation experiments were carried out by installing perforated walls along the exit of the scaled tunnel simulator. Firstly, the effect of perforated walls on the suppression of overpressures of the shock waves was confirmed. Secondly, a similar arrangement to the scaled tunnel simulator was tested in a 9 km long tunnel on the Tohoku Shinkansen. Good agreement was obtained between the laboratory scale experiment and the real tunnel measurement. In this paper, a recent result of the reduction of train tunnel sonic booms is reported.

2. Apparatus

A piston moving along a tube induces shock waves in the tube. If the viscosity is neglected during the process of shock wave formation, the governing equations are given by the unsteady Euler equations in which no characteristic length exists. This implies that the wave motion will be analogous to flows having the identical flow velocity in the scaled geometry. In relation to the present train tunnel problem, if a scaled train model moves along a scaled tunnel with the identical train speed as the real one, the overpressure of the shock waves which will be created ahead of the scaled train model will be identical to those occurring in the real train tunnel.

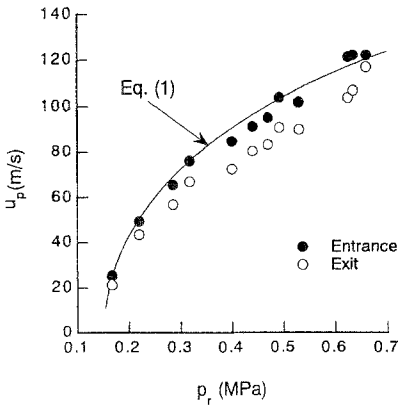

Fig. 3. Piston speed *vs.* reservoir pressure. Filled circles and open circles show piston speed at the entrance and the exit of the tunnel simulator, respectively

In order to simulate train tunnel sonic booms in the laboratory, it was decided to launch a piston which is a plastic model train into a long tube along which it moves hopefully at a constant speed. Figure 1 shows a 1 : 300 scaled train-tunnel simulator at the Shock Wave Research Center, Institute of Fluid Science, Tohoku University. This train tunnel simulator consists of a driver section, an acceleration tube, a sabot separator, a test section and a piston recovery section. The train tunnel simulator was inclined at approximately 8° to the floor so as to make the gravitational force created by this inclination cancel the drag force caused by friction from the direct contact between the steel tube and the plastic piston. Hence, as seen later, piston speeds at the entrance were nearly maintained constant throughout the length of the train tunnel simulator.

At the driver section, pressurized nitrogen at 0.2 to 0.7 MPa was supplied to the driver gas reservoir. The 25 mm dia. and 3.8 m long acceleration tube followed the gas reservoir. An 18 mm dia. and 200 mm long cylindrical piston made from nylon was supported by 25 mm dia. sabots at its front and rear ends. The front sabot had a breakable structure and the rear sabot was a solid piece.

The piston was 50 g in weight and its total weight including these sabots was 80 g. The piston supported by the sabots was inserted at the end of the acceleration tube as seen in Fig. 2. The high pressure driver gas and the acceleration tube were separated by one or two 9 to 25 μm thick Mylar diaphragms. By mechanically piecing the diaphragm, the driver gas started to accelerate the piston and the sabots (Sasoh et al. 1994a, 1994b).

Figure 3 shows the performance of the driver section, that is, a relationship between the experimental piston speeds up at the entrance of the test section and the driver gas pressure. The piston speed increases monotonically with increase of the driver pressure p_r. At the driver gas pressure of 0.7 MPa, the piston speed is approximately 120 m/s. The performance of the driver section was formulated by Sasoh et al. (1994b)

$$u_p = u^* \sqrt{\frac{\beta - 1 - \alpha_f}{1 + c\beta}}, \tag{1}$$

where c is a constant to be determined by data fitting, α_f is the ratio of the estimated piston-wall friction force to the product of the atmospheric pressure and the cross sectional area of the sabots, and β is the ratio of the driver gas pressure to the atmospheric pressure. u^* is given by

$$u^* = \sqrt{\frac{2p_0 A_p l_a}{m_p}}, \tag{2}$$

where A_p, l_a, m_p, and p_0 are the cross sectional area of the sabots, the length of the acceleration tube, the total mass of the piston and sabots and the atmospheric pressure, respectively.

As seen in Fig. 2, a sabot separator which had a conically shaped entrance was placed in the position facing the exit of the acceleration tube. The front sabot was breakable into 4 pieces when it impacted at the edge of the conical entrance of the sabot separator while the rear sabot had a conical opening at its front face which enabled the rear sabot to plug in at the conical entrance of the sabot separator. This was designed to stop the high pressure driver gas from overtaking the piston and eventually entering into the test section where it may consequently produce a undesired shock wave. Between the exit of the sabot separator and the entrance of the test section, a 0.4 m long half open section was set which was intended to disconnect the influence of the sabot separator and the acceleration tube from the motion of the piston in the test section.

The test section was a 40 mm dia. approximately 25 m long steel tube which was composed of seven tubes each 3.4 m long and a 1.2 m long tube. These segments were flanged to each other. This test section could, therefore, simulate a real tunnel of 7.5 km in length. The ratio of the cross section of trains to that of the real tunnel is known to be approximately 0.20 so that, in this experiment, the value of the experimental area ratio between the plastic piston and the test section was selected to be the same as the real tunnel. Real tunnels have double tracks and their shape is not necessarily a circular shape. However, in the present tunnel simulator, the piston slides along the wall of the circular tube. It is considered that these geometrical differences will not cause any significant discrepancies when results obtained in the present tunnel simulator were compared with those of real tunnels.

It should be noticed that the present tunnel simulator has a smooth wall surface, whereas real tunnels have significant wall surface roughness. This effect will be discussed later. Seven pressure transducers (Kistler 603B) were distributed along the test section at 3.4 m equi-distances as shown in Fig. 1. The measured pressure histories were recorded by two transient recorders (Iwatsu DM7200) and afterwards displayed on a personal computer. In Fig. 3, filled and open circles show piston speeds at the entrance and the exit of the tunnel simulator, respectively.

The piston speed at the exit was attenuated by approximately 10 % at u_p = 120 m/s. The discrepancy of the piston speed between the entrance and the exit tends to become noticeably large with increase of the piston speed. The piston decelerates due to drag forces, such as the friction between piston and wall and the aerodynamic drag force. The present

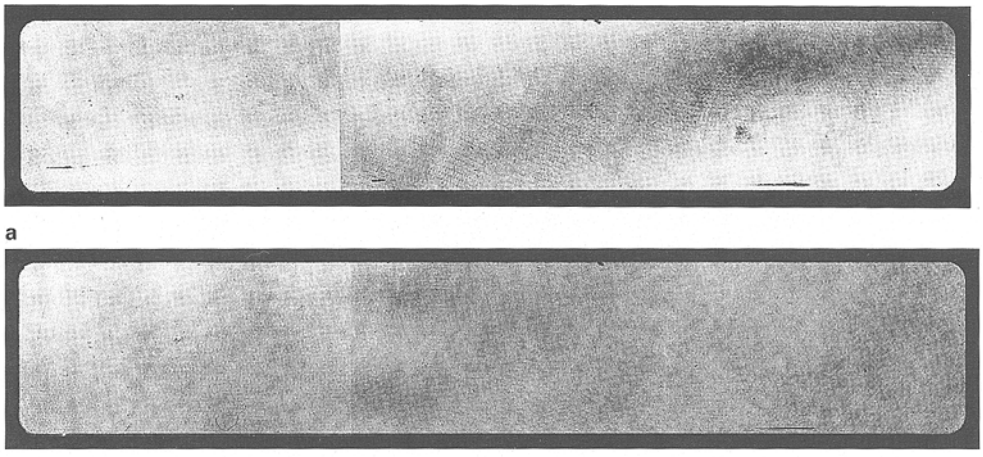

Fig. 4a,b. Shock waves in the tunnel simulator: **a** u_p = 75 m/s; and **b** u_p = 60 m/s

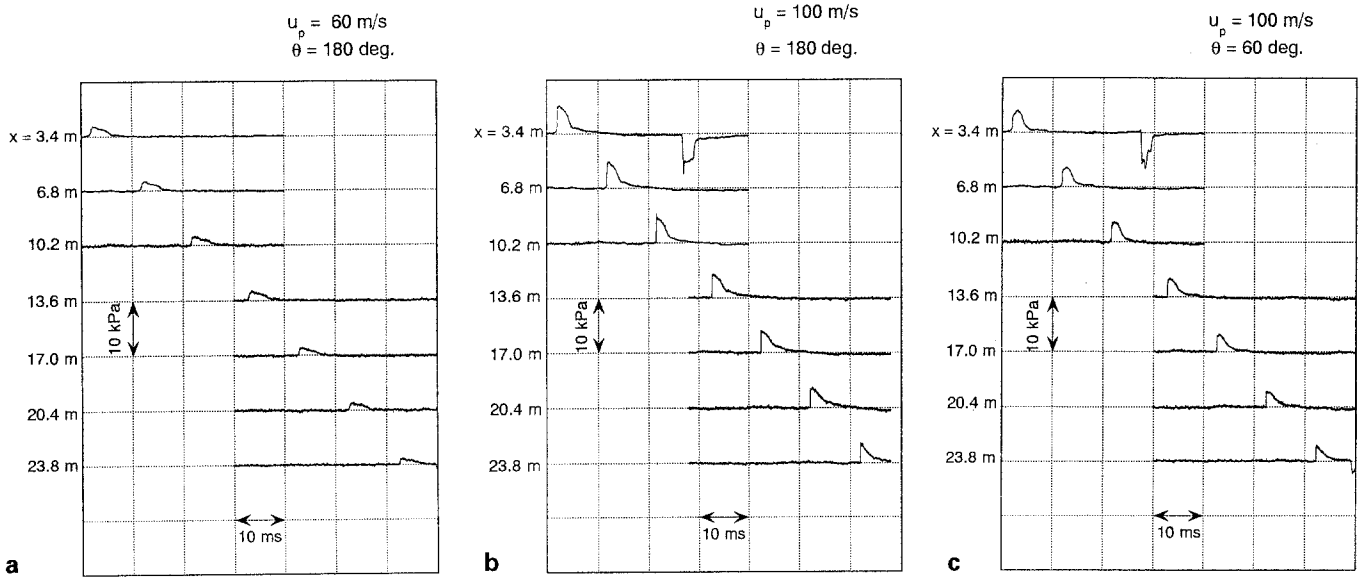

Fig. 5a–c. **a** Overpressure histories, u_p = 60 m/s, θ = 180°; **b** Overpressure histories, u_p = 100 m/s, θ = 180°; and **c** Overpressure histories, u_p = 100 m/s, θ = 60°

train tunnel simulator was inclined by 8 degrees so that the friction between the piston and the wall is nearly canceled by the tangential component of the gravitational force. Only the aerodynamic drag can then decelerate the piston. Sasoh et al. (1994b) estimated the deceleration of the piston caused by the aerodynamic drag and found it to be 15 %. The experimental value was found to be close to this value.

For flow visualization purposes, a 30 mm × 40 mm rectangular observation section was connected to the end of the test section (Takayama et al. 1993; Sasoh 1994a; 1994c). Its cross sectional area is nearly the same as the 40 mm dia. test section. For the reduction of shock overpressures, 40 mm dia. and 0.5 m long tubes having various inner wall conditions such as perforated walls or slotted walls were connected to the end of the test section. Pistons which were released from the exit of the test section were recovered as shown in Fig. 1 by catching them with a stopper which consisted of thick layers of inserted sponge sheets.

3. Generation of shock wave

Figure 4a and 4b shows shock waves which appeared in the present tunnel simulator at piston speeds of u_p = 75 m/s (270 km/h) and 60 m/s (216 km/h), respectively. The optical flow visualization was conducted by using double exposure holographic interferometry (Takayama et al. 1993; Sasoh et al. 1994c). The shock wave in Fig. 4a appears to be discontinuous and, as seen later, its overpressure is approximately 1.8 kPa, with a corresponding shock wave Mach number Ms is approximately 1.009. The change in the contrast across the shock wave driven in Fig. 4b is not as clear as that by a 75 m/s piston. In Fig. 4b, the shock overpressure is approximately 1.0 kPa and its corresponding shock Mach number is only 1.004. Hence the shock wave appears to be slightly smeared with a structure that is, although not exactly, analogous to that of partially dispersed shock waves. It is reported that the human audibility perception of sonic booms is related to the time variation of the

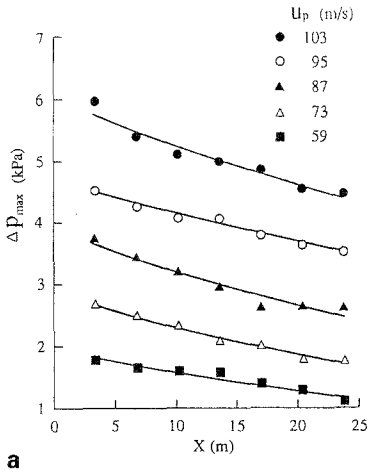

a

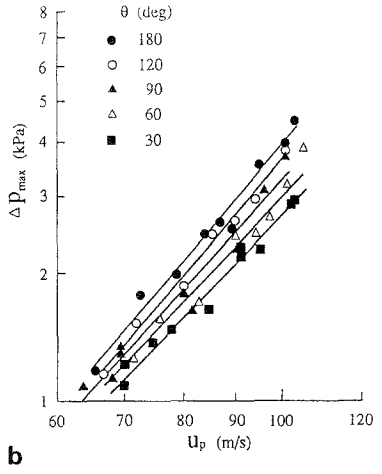

b

Fig. 6a,b. **a** Δp_{max} *vs.* x; and **b** Δp_{max} *vs.* u_p

peak pressure (Matsuo and Aoki 1992). Therefore, the sonic boom created by train speed of 60 m/s becomes less loud to human audibility than that of 75 m/s operation. Incidentally, this fact fairly agrees well with observations of sonic booms created by real train tunnels, that is, the tunnel sonic boom becomes louder for a train speed of more than 67 m/s whilst it is not so significant for that of less than 60 m/s.

Figure 5a to 5c shows time variations of shock overpressures measured at various positions x along the test section. The effect of the frontal shape of the piston was examined where θ is an apex angle of the conically shaped pistons. The apex angle of $\theta = 180°$ corresponds to a flat faced piston and $\theta = 60°$ shows a conically faced piston. Figure 5a shows the case of $u_p = 60$ m/s and $\theta = 180°$. Upon the train entrance into the test section, compression waves were built up in front of the piston and were already a maximum at $x = 3.4$ m. At approximately 25 ms after the arrival of the compression waves at the pressure transducer, a negative pressure wave is observed which corresponds to the arrival of the piston at the position of the pressure transducer. The time interval between the arrival of compression waves or a shock wave and the negative pressure therefore indicates a stand-off distance between the shock wave and the piston which increases with the lapse of time and is not displayed in other pressure recordings. Although the head of the compression wave is gradually steepened with propagation, the peak value of the compression wave is gradually decreased. This effect will be discussed later in Fig. 6

Compression waves formed ahead of a piston are a simple wave (Shapiro 1983). The shock formation distance is inversely proportional to the pressure gradient of the head of the simple wave. For the low piston speed in Fig. 5a, the time derivative of the head of compression waves remains finite throughout the test section. Figure 5b shows the time variation of pressure recorded at various stations for the piston speed of $u_p = 100$ m/s with the flat piston face of $\theta = 180°$. It is readily observable that compression waves coalesce, with propagation, into a shock wave. However, although the rise time of shock wave overpressures is discontinuous, the rise time of the measured shock wave overpressures is found to be finite due to the finite size of the pressure transducers.

Figure 5c shows the time variation of the pressure recording at various stations at $u_p = 100$ m/s and for $\theta = 60°$. Due to the sharp conical face of the piston, the pressure variation at $x = 3.4$ m shows a gradual increase which delays the transition of compression waves into a shock wave. The frontal shape of the piston is, therefore, found to affect the process of formation of tunnel sonic booms. The peak overpressure of compression waves generated ahead of a sharpened piston is relatively low. The frontal shape, as seen later, influences not only the formation of the final peak overpressures but also their rise time.

Figure 6a shows a relationship between the peak shock wave overpressure Δp_{max} in kPa along the test section length x for a piston speed ranging from 59 m/s to 103 m/s measured at the exit. The peak shock wave overpressure is a maximum at the entrance and monotonically decreases with x and increases with increase of piston speed. This trend agrees with the observation shown in Fig. 5. In Fig. 6b, the ordinate is Δp_{max} in kPa and the abscissa is u_p in m/s. The value of Δp_{max} is compared with u_p for various apex angles of conical piston faces. The overpressure behind a weak planar shock wave is related to the shock wave Mach number Ms as follows,

$$\Delta p_{max}/101.3 = 2.33(Ms - 1) \quad \text{for} \quad \gamma = 1.40. \tag{3}$$

In reality, Δp_{max} may not be constant behind weak shock waves but may be slightly attenuated due to the shock attenuation caused by the wall boundary layer which develops behind the shock wave. Equation (3) can predict shock wave Mach numbers for measured shock overpressures. The apex angle of the conical piston face significantly affects the shock wave overpressure for higher piston speeds. Within the scatter of measured peak shock wave overpressures, it is found that Δp_{max} at $u_p = 100$ m/s for a piston having a $\theta = 30°$ conical front face is only 65 % of that created by the flat faced piston.

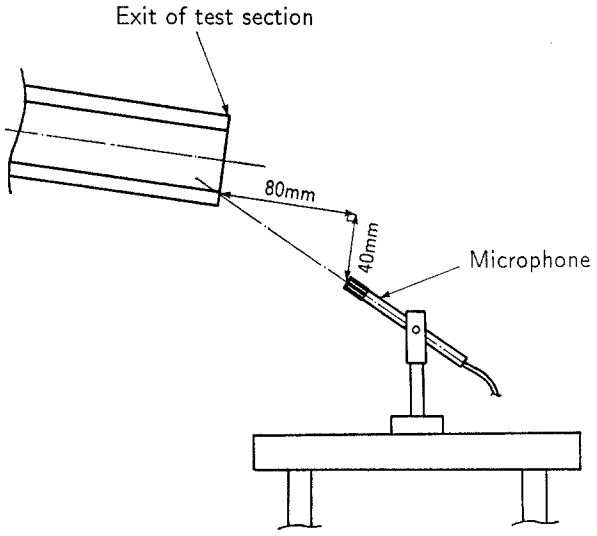

Fig. 7. Arrangement of overpressure measurement by using a microphone at the exit of the test section

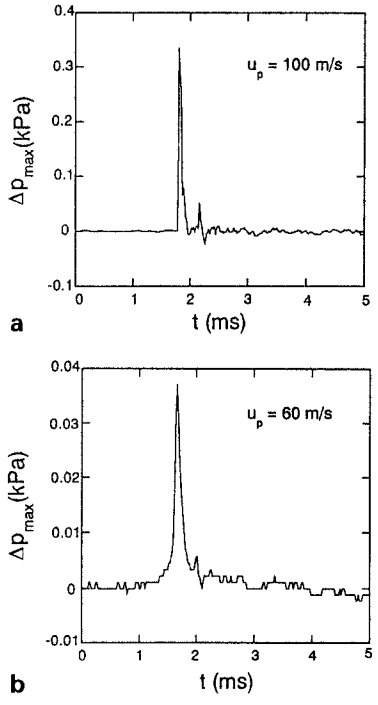

Fig. 8a,b. Time variations of overpressures measured by the microphone at the exit of the test section; **a** u_p = 100 m/s; and **b** u_p = 60 m/s

4. Reduction of tunnel sonic booms

When a simple compression wave is emitted from the exit of the test section, an impulsive pressure wave is generated. Then the overpressure of the impulsive wave is proportional to the time derivative of the pressure variation at the exit of the tube (Rudinger 1957; Stollery et al. 1981; Kashimura et al. 1994). However, this relation does not hold in the case of shock waves. The evaluation of peak overpressures of the impulsive sound wave is related to its energy flux and the peak overpressure. The overpressures can well define the strength of the sonic boom.

In the present experiment, the strength of the sonic boom was defined by an overpressure measured, at a point shown in Fig. 7, by using a capacitor-type microphone (Brüel and Kjær 4135). This microphone has a high sensitivity and a high S/N ratio. Its gain performance is ±0.3 dB under 5 kHz and ±2.0 dB under 100 kHz. Figure 8a and 8b shows time variations of shock overpressure measured at the point as shown in Fig. 7. When emitted from the open end of the tunnel simulator, the shock wave is diffracted at the edge of the open end. The shock overpressure Δp_{max} is measured by this microphone positioned in a head-on mount at two characteristic distances along the x-direction and one characteristic distance along the y-direction as shown in Fig. 7. In the case of high piston speed, for example at u_p = 100 m/s, Δp_{max} is approximately 350 Pa as shown in Fig. 8a. At u_p = 60 m/s, the wave front has a finite pressure gradient as seen in Fig. 8b and the peak overpressure Δp_{max} is now 38 Pa.

4.1. Entrance hoods

Ozawa (1979) confirmed the effect of installation of a hood at the entrance of a tunnel on the reduction of the overpressure of the impulsive sound wave. In the case of lower overpressures, compression waves will never coalesce into a shock wave as seen in Fig. 5a. In this particular case, the installation of an entrance hood was found to be effective. Iida (1993) conducted a numerical simulation of the entrance hood and showed that the build-up of compression waves was well suppressed by its installation. Indeed, in some of the Shinkansen tunnels, entrance hoods have been often used for suppression of tunnel sonic booms. The effect of entrance hoods was tested for the first time by using the train tunnel simulator designed for high-speed piston entrance by Ozawa et al. (1976).

The shape of entrance hoods under study is sketched in Fig. 9. Let a type-A model be a control one, which is a 65 mm dia. and 115 mm long co-axial half-cylinder. A type-B model has an identical cross section to the type-A model but is twice as long. A type-C model is 115 mm long but its diameter is 80 mm. A type-D model has a 115 mm long conical configuration with an entrance of a 65 mm dia. which gradually converges to a diameter of 40 mm. These entrance hood models were successively installed at the entrance of the test section.

All overpressures shown in Fig. 10 were measured at 13.6 m from the entrance at a train speed of 70 to 73 m/s. Figure 10a–c show pressure histories corresponding to the type-A entrance hood, that of the type-D entrance hood, and that without using any entrance hood, respectively. When a piston enters into the test section which has a sudden two step area contraction at its entrance, compression waves were built up at the steps as seen in Fig. 10a. Hence, the rise of compression wave heads became more gradual and the profile of the compression waves had two maxima. A similar trend was observable in the case of a gradual area contraction of the type-D model. Therefore, the coalescence of compression waves into a shock wave would be significantly delayed. However, the pressure rise in the case of the type-D model was found to be steeper than that in the type-A model. This indicates that the

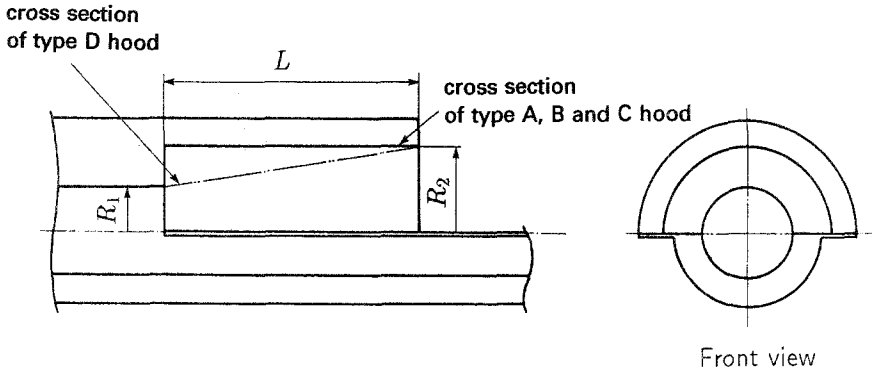

Fig. 9. Configuration of various entrance hoods

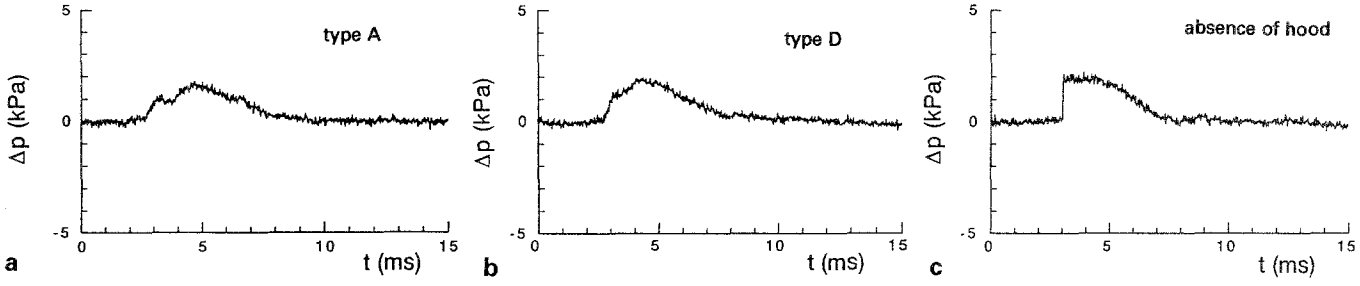

Fig. 10a–c. Time variation of overpressure for piston speed 70–73 m/s: **a** type-A entrance hood; **b** type-D entrance hood; and **c** in the absence of any entrance hood

type-D model is less effective for the suppression of the formation of shock waves. The steeper pressure variation in the absence of entrance hoods shown in Fig. 10c, which, unlike that of Figs. 10a and 10b, obviously showed the generation of shock waves. It is concluded that the entrance hood in the type-A model is effective for the suppression of shock wave formation.

Figure 11a shows pressure distributions of one-dimensional planar shock waves whose propagation speed is U_A. The states 1 and 2 represent conditions in front of and behind the shock wave, respectively. The effect of entrance hoods is illustrated by taking into account two weak shock waves propagating in the same direction. The second shock wave is overtaken by the first as seen in Fig. 11b. The pressure distribution of these two shock waves B and C is shown in Fig. 11b. The state between B and C is labeled by 1'. The shock wave C propagates faster than the characteristic speed of $u_{1'} + a_{1'}$ where a is the speed of sound of air and u the particle velocity behind the shock wave B. When the shock wave C eventually catches up to the shock wave B, assuming that the total overpressures of B and C are equal to each other, $p_{1'}$ is determined as,

$$p_{1'} = P_1 + \alpha \Delta p, \quad (0 < \alpha < 1), \tag{4}$$

From the Rankine-Hugoniot relations,

$$M_A = \sqrt{\frac{\gamma + 1}{2\gamma} \frac{\Delta p}{p_1} + 1}, \tag{5}$$

$$M_B = \sqrt{1 + \alpha(M_A^2 - 1)}, \tag{6}$$

$$M_C = \sqrt{\frac{(1 - \alpha)(M_A^2 - 1)}{1 + 2\gamma\alpha(M_A^2 - 1)/(\gamma + 1)} + 1}, \tag{7}$$

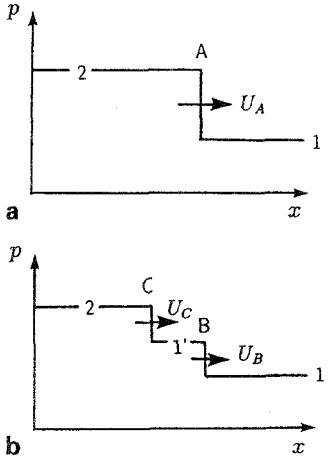

Fig. 11a,b. Pressure distribution: **a** a single shock wave; and **b** two shock waves propagating in the same direction

where M_A and γ denote the Mach number and the specific heats ratio, respectively.

$$\Delta U = U_C - U_B, \tag{8}$$

where $U_B = a_1 M_B$ and $U_C = u_{1'} + a_{1'} M_C$ and $a_{1'}$ and $u_{1'}$ are given by the Rankine-Hugoniot relations and are expressed as a function of M_B.

Substituting typical values of $\Delta p/p_1 = 2 \times 10^{-2}$ and $\alpha = 0.5$ into (5) to (6), ΔU in (8) is then given as 2.9 m/s. Therefore, the time, $\Delta t|_c$, for the shock wave C to catch up to the shock wave B is estimated to be approximately 40 ms. The time duration $\Delta t|_s$ for the shock wave to pass through the entire test section is approximately 73 ms, which is comparable with $\Delta t|_c$. For low piston speeds, $\Delta t|_c$ is longer than $\Delta t|_s$. Under such conditions, the pressure gradient will remain finite so that

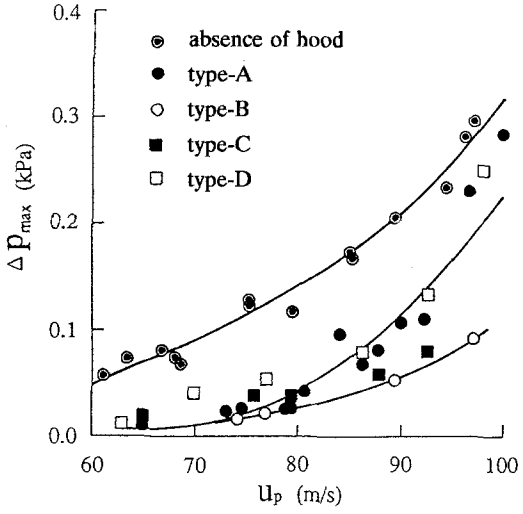

Fig. 12. Comparison of Δp_{max} for various entrance hood configurations

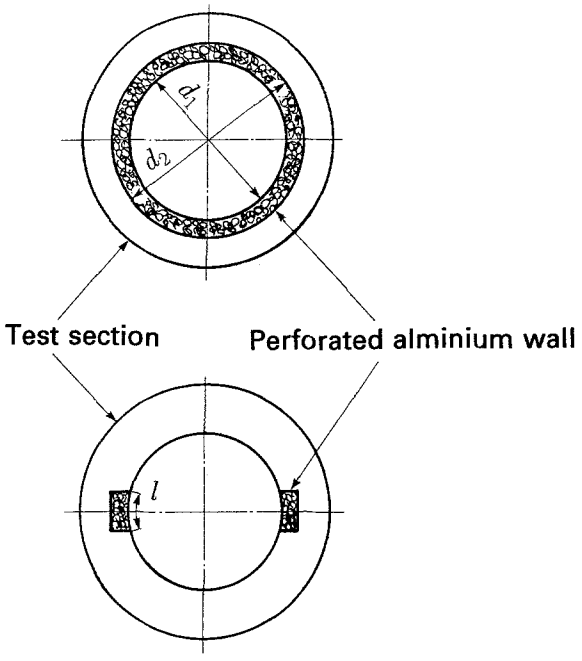

Fig. 13. Perforated wall

the coalescence of compression waves into a shock wave can be subsequently retarded. This obviously reduces the strength of tunnel sonic booms.

In Fig. 12 the effect of these four types of entrance hoods on peak shock wave overpressures are compared for u_p values ranging from 60 to 100 m/s. The ordinate is the peak shock wave overpressures measured by a microphone place at the exit of the test section as shown in Fig. 7 and the abscissa is u_p. Open circles with a dot inside designate shock wave overpressures in the absence of any attached entrance hood, filled circles show results with the type-A model attached, open circles are with the type-B model, filled squares with a white dot inside are with the type-C model and open squares with the type-D model. The remarkable effect of suppression on peak shock wave overpressures can be seen in general when hoods were attached at the tunnel entrance. Type-B and C models indeed show favorable suppression of the peak shock wave overpressures, whereas the suppression caused by type-A and D models is, although of similar trend, less effective than type-B and C models. For u_p lower than 70 m/s, shapes of the entrance hoods do not affect the suppression of peak shock wave overpressures.

For high u_p, the type-A model appears to be less effective. With increasing u_p, α becomes close to unity so that the effect of the entrance hood becomes smaller. However, by enlarging the cross section of the entrance hood, α becomes smaller. Consequently, a larger diameter hood such as the type-B model and an elongated entrance hood such as the type-C model can readily suppress the peak shock wave overpressure much effectively even at higher u_p. The type-D model has a conical shape and shows similar characteristics to the type-A model.

As discussed above, the installation of an entrance hood created two simple waves successively corresponding both to the first entrance hood and to the the entrance of the test section. Before the compression wave C to catch up the compression wave B, $t \leq \Delta t|_c$, these two simple waves do not merge so that their coalescence into a shock wave will be delayed. Since with increase of u_p α will tend to increase toward unity, generally speaking, the entrance hood becomes less effective for the suppression of the peak shock wave overpressure. On the contrary, it becomes more effective for low u_p.

4.2. Effect of wall perforations

It is known that if a shock wave passes through a porous or perforated wall, the mass suction through the perforated wall subsequently induces a loss of momentum and energy fluxes and thereby decreases the shock wave strength (Wu and Ostrowski 1971; Szumowski 1971; Deckker and Koyama 1983; Onodera and Takayama 1990; 1992). The effect of shock wave attenuation along perforated shock tube walls was then applied to suppress tunnel sonic booms. Figure 13 shows a perforated aluminum wall which has a structure similar to a sponge but made from aluminum and which covered partially or completely the inner surface of the test section. This perforated aluminum wall has a density and porosity of from 0.2 to 0.3 and about 0.9, respectively. The thickness of the perforated aluminum wall was approximately 5 mm. As seen in Fig. 13, if the perforated aluminum wall of width ℓ was placed on the side walls of the tunnel simulator, the coverage of the perforated wall over the circumference of the test section can be represented by a ratio b which is defined as 2ℓ divided by πd_1, where d_1 is diameter of the test section. In the present experiment, cases of b = 1.0, 0.16, and 0 were tested.

Figure 14a and 14b shows overpressure histories which were measured for u_p = 98 m/s and 65 m/s along a perforated aluminum wall installed completely around the circumference of the test section πd_i. The distance x' was measured from the perforated part of the test section. It is found that a shock wave was already at $x' = -0.67$ m before entering into the perforated section. When the shock wave passed through the perforated section, due to mass out flow through the perforations,

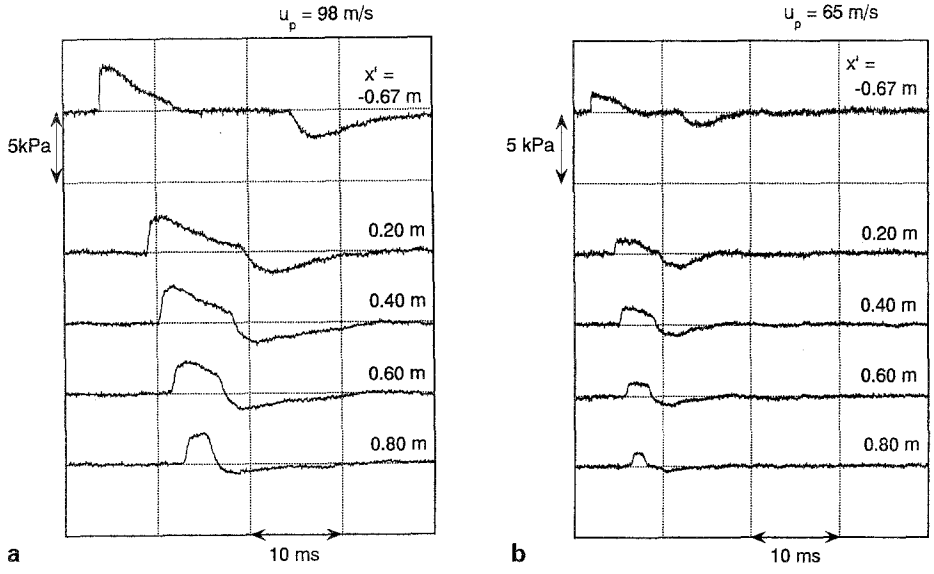

Fig. 14a,b. Time variations of overpressures along perforated aluminum walls, $b \simeq 1.0$; **a** u_p = 98 m/s; and **b** u_p = 65 m/s

expansion waves were generated at individual holes of the perforated wall. These expansion waves hence overtook the shock wave from behind and attenuated it (Onodera and Takayama 1992). As a result, the initial shock wave overpressure was lowered and, with further propagation, even the initial steep rise of the overpressures became smeared. This trend is more pronounced for higher piston speeds as shown in Fig. 14a. It is noted that a negative pressure profile is induced by a centered expansion fan reflected from the exit of the test section. Being superimposed by the incident simple wave, the level of the negative pressure near the exit of the test section is small. In the pressure profile at x' = -0.67, these two waves were completely separated from each other.

Figure 15 shows the effect of b. Peak overpressures Δp_{max} were measured for various u_p values by a microphone placed at the exit of the test section as shown in Fig. 7. Filled circles show results in the absence of the perforated wall, b = 0, filled squares correspond to the case of the complete coverage of the inner wall with the perforations, b = 1.0, and open circles correspond to the case of b = 0.16 in which only 16 % of the circumference was covered by the perforation. Complete coverage with the perforated wall, b = 1.0, as seen in Fig. 14a,b, decreases Δp_{max} significantly at higher piston speeds. The peak overpressure Δp_{max} in the case of b = 1.0 was approximately one third of that in the absence of the perforated wall. The value of Δp_{max} in the case of b = 0.16 for u_p = 100 m/s was approximately two thirds of that obtained in the absence of the perforated wall. This implies that, in applying the perforated walls to real train tunnels, there will be practically no need to completely cover the tunnel inner walls with perforations.

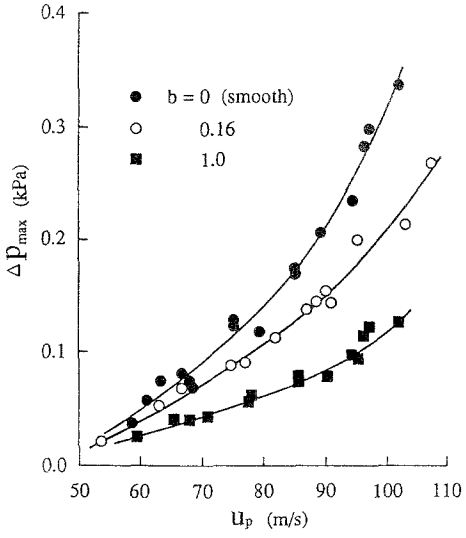

Fig. 15. Effect of the ratio of coverage of perforated wall, b, for suppression of Δp_{max}

4.3. Combination of entrance hood and perforated wall

As seen in Sections 4.1 and 4.2, entrance hoods are found to effectively suppress the steepening of compression waves particularly for low piston speeds whereas perforated walls can attenuate shock waves created at higher piston speeds. Therefore, in order to reduce tunnel sonic booms in the tunnel simulator, a hood was installed at the entrance of the test section and simultaneously a perforated wall of b = 0.16 was placed at the end of the test section. Figure 16 shows the relationship between Δp_{max} and u_p for the combination of a type-A model entrance hood and a perforated wall with b = 0.16. Peak overpressures were measured again by a microphone shown in Fig. 7. Filled circles show results in the absence of the entrance hood and the perforated wall. These data points are same ones as the filled circles in Fig. 15. Filled squares show results with the type-A model entrance hood, which are same ones as the filled circles in Fig. 12. The open circles show results for the perforated wall of b = 0.16, which are shown by the open circles in Fig. 15. Open squares show a combination of the type-A model entrance hood and the perforated wall with b = 0.16.

It is readily found that the combination of the type-A model entrance hood and the perforated wall with b = 0.16 effectively suppresses shock wave overpressures for a wide range of piston speed from u_p = 55 m/s to 105 m/s. As abovementioned, the perforated wall is found to effectively attenuate shock waves especially for high piston speeds. For low piston

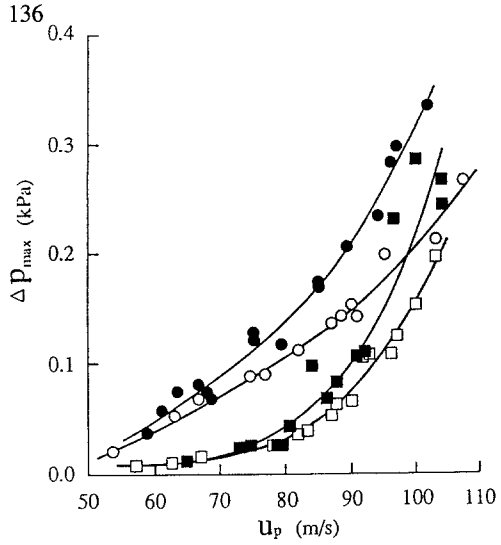

Fig. 16. Effects of the entrance hood and/or perforated wall on shock wave overpressure reduction: • $b = 0$ and absence of entrance hood; ○ $b = 0.16$ and absence of entrance hood; ■ $b = 0$ and type-A hood; and □ $b = 0.16$ and type-A hood

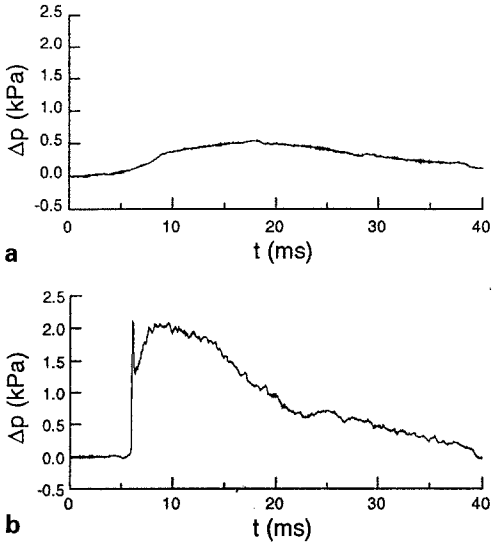

Fig. 17a and b. Pressure measurements in a real train tunnel in the absence of the wall perforation: **a** 205 km/h; and **b** 245 km/h

speeds, the pressure gradient of the head of the compression waves remains to finite even in the absence of wall perforations. Combining simultaneously the type-A model entrance hood and the perforated wall, the peak overpressure Δp_{max} was decreased by 50 to 80 % of that obtained in the absence of the entrance hood and the perforated wall.

4.4. Real tunnel experiments

In order to verify the effectiveness of the abovementioned wall perforation applied to the tunnel simulator, pressure measurements were carried out in a 9 km long tunnel of Tohoku Shinkansen. Pressure transducers used for this measurement consist of a 24 μm thick and approximately 50 mm dia. PVDF film (Polyvinylidenefluoride Piezo Film, Solvey Co. Ltd.) and were manufactured and calibrated in-house. The PVDF film was sandwiched between a 0.3 mm thick and 70 mm dia. aluminum diaphragm and a 50 mm dia. brass cylinder and was accommodated in a brass housing. The aluminum diaphragm face to the air and the brass cylinder were electrically insulated from the housing metal. The pressure transducer was positioned vertical towards the tunnel wall at 1.5 m from the exit of the tunnel facing to the tunnel entrance. Therefore, the present pressure transducer could measure only the pressure behind the reflected shock wave.

Upon the impingement of shock waves on the pressure transducer, corresponding output signals were stored on a transient recorder and later displayed on the monitor of a personal computer. Pressure transducers were calibrated against overpressures of blast waves which were generated by microexplosions of 10 mg silver azide pellets. The distance-overpressure curve of blast waves caused by these explosions has already been obtained. Hence, the sensitivity of the PVDF pressure transducer could be readily calibrated with a reasonable accuracy by comparing the output of the PVDF pressure transducer placed at a given stand-off distance with this distance-overpressure curve of the silver azide pellets.

The pressure histories obtained by using this PVDF pressure transducer which was installed in the tunnel are shown in Fig. 17a–d. Pressure measurements were conducted for two types of train configurations. Figure 17a shows a pressure history measured. The pressure rise of the compression wave appears to be gradual for a train speed of 205 km/h and hence its overpressure is low, whereas a steep pressure rise at the shock wave can be seen in Fig. 17b for a train speed of 245 km/h. The shock wave overpressure in Fig. 17b is approximately 2.0 kPa. Since the frontal surface of the pressure transducer was facing towards the shock wave, the measured shock wave overpressure corresponds to the pressure behind the reflected shock wave. The true peak overpressure behind the incident shock wave is nearly one half of the measured reflected pressure. The incident shock wave reflected, hence, diffracted at the margin of this disk shaped pressure transducer. The measured peak pressure was continuously decreased due to the overtaking expansion wave generated at the margin.

Due to the large diameter of the PVDF pressure transducer surface, it took approximately 75 μs after the impingement of the incident shock wave for the expansion wave from the edge of the pressure transducer to merge at the center. At that time a minimum pressure is achieved. Soon after this occurrence, the pressure recovers to the peak value and the peak overpressure plateau appears. However, the pressure decrease commences at approximately 10 ms after the shock impingement on the pressure transducer.

Encouraged by the result of perforated walls, two perforated aluminum walls which were each 30 mm thick, approximately 1.5 m wide and 200 m long were placed on the side wall of the tunnel. Consequently the perforated aluminum wall covered approximately 17 % of the inner circumference of this tunnel. The identical pressure transducer was used both for perforated aluminum walls and the normal tunnel wall. For slower train speeds, the reduction of peak overpressures was

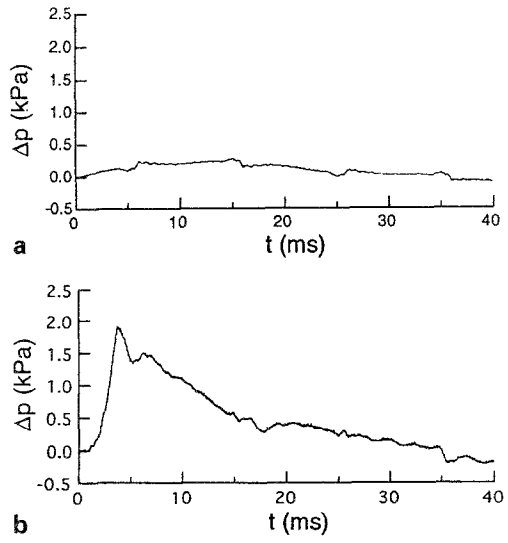

Fig. 18a and b. Effect of wall perforation. Pressure measurement in a real train tunnel: **a** 205 km/h; and **b** 240 km/h

not observed as seen by comparison between Figs. 17a and 18a.

5. Conclusions

Results of a scaled train tunnel simulator are presented in order to experimentally clarify the generation of tunnel sonic booms and to find an effective method of suppression of the tunnel sonic booms. The results obtained are summarized as following:

(1) Upon the entrance of a high-speed piston in the test section of the tunnel simulator, waves generated in front of the piston are a simple wave, which eventually coalesces into a shock wave. This occurs for a high piston speed and a reasonably long test section.

(2) The installation of an entrance hood at the test section indeed delayed the formation of shock waves. This effect is significant for relatively slow piston speed such as $u_p = 60$ to 80 m/s.

(3) By installing a porous wall at the exit of the test section, the gradient of the shock wave overpressure became less steep indicating that the wall perforation effectively attenuated the shock waves. This amount depended upon the ratio of coverage of the perforated wall on the tunnel simulator. This effect is particularly pronounced for higher piston speeds over 80 m/s.

(4) Consequently the combination of an entrance hood and perforated wall can very effectively decrease the shock overpressures for a wide range of piston speeds of $u_p = 60 \sim 100$ m/s.

(5) Results were examined in a real train tunnel by installing on the tunnel side wall, two layers of perforated walls, 1.5 m wide and 200 m long each. It was found that the perforated wall of area coverage of approximately 20 % indeed decreased the shock overpressure by approximately 30 %. The effect of these perforated walls on the suppression of the shock overpressures was less pronounced for slower trains.

Acknowledgements. The authors would like to thank Messrs H. Ojima and T. Ogawa of the Shock Wave Research Center, Institute of Fluid Science, Tohoku University, for their assistance in conducting the present experiments.

References

Aoki T, Kashimura H, Nonaka Y, Matsuo K (1992) Discharge of a compression wave from an open end of a tube. In: Takayama K (ed) Shock Waves, Proc. of the 18th Intl. Symp. on Shock Waves. Springer-Verlag, Heidelberg, pp 1331–1334

Blake WK (1986) Mechanics of flow-induced sound and vibration, vol. 1. Academic Press, p 204

Deckker BEL, Koyama H (1983) Motion of a weak shock wave in a porous tube. In: Archer, Milton (eds) Proc. 14th Intl. Symp. Shock Tubes Waves, Sydney pp 239–246

Iida M (1993) Numerical studies of compression waves generated by train entering tunnels. Ph.D thesis, Univ. Tokyo

Kasimura H, Yasunobu T, Aoki T, Matsuo K (1994) Emission of a propagating compression wave from an open end of a tube (2nd Report, relation between incident compression wave and impulsive wave). Tran. Jpn Soc. Mech. Engineers (in Japanese) B60:71

Lukasiewicz J (1976) Rail way game. Carlton Contemporary

Matsuo K, Aoki T (1992) Wave problems in high-speed railway tunnels. In: Takayama K (ed) Shock Waves, Proc. of the 18th. Intl. Symp. on Shock Waves. Springer-Verlag, Heidelberg, pp 95–102

Onodera H, Takayama K (1990) Shock wave reflection over wedges with suction. Tran. Jpn Soc. Mech. Engineers (in Japanese) B56:112

Onodera H, Takayama K (1992) An analysis of shock wave propagation over perforated wall and its discharge coefficient. Tran. Jpn Soc. Mech. Engineers (in Japanese) B58:1408

Ozawa S, Moritoh Y, Maeda T, Kinoishita M (1976) Investigation of pressure wave radiated from a tunnel exit (in Japanese). Railway Tech Res Rep, The Railway Tech Res Inst, Japan Nat Railways 1023

Ozawa S (1979) Studies of micro-pressure wave radiated from a tunnel exit. Railway Tech Res Rep, The Railway Tech Res Inst, Japan Nat Railways 1121

Rudinger G (1957) The reflection of pressure waves of finite amplitude from an open end of a duct. J. Fluid Mech. 3:48

Sajben M (1971) Fluid Mechanics of train-tunnel systems in unsteady motion. AIAA J 9:1538-1545

Sasoh A, Onodera O, Takayama K, Kaneko R, Matsui H (1994a) Experimental study of shock wave generation by high speed train entrance in to a tunnel (in Japanese). Trans Jpn Soc Mech Engineers, in press

Sasoh A, Onodera O, Takayama K (1994b) Scaled train-tunnel simulator for weak shock wave generation experiment. Rev. Sci. Instrum. 65:3000

Sasoh A, Funabashi S, Saito T, Takayama K (1994c) A numerical and experimental study of sonic boom generated from high speed train tunnels. In: Proc of the 19th Int Symp on Shock Waves. Springer-Verlag, Heidelberg, in press

Sasoh A, Onodera O, Takayama K, Kaneko R, Matsui H (1994d) Experimental investigation of the reduction of railway tunnel sonic boom (in Japanese). Trans Jpn Soc Mech Engineers, submitted

Shapiro AH (1983) The Dynamics and Thermodynamics of Compressible Fluid Flow, vol. 2. Robert E Krieger Publ, Reprint Edition

Stollery JL, Phan KC, Garry KP (1981) Simulation of blast waves by hydraulic analogy. In: Treanor CE, Hall JG (eds) Shock Tubes and Waves, Proc. 13th Intl. Symp., pp 781–786

Szumowski AP (1971) Attenuation of a shock wave along a perforated tube. In: Stollery JL, Gaydon AG, Wen PR (eds) Shock Tube Research, Proc. 8th Int. Symp. Shock Tubes. Chapman & Hall 14

Takayama K, Saito T, Sasoh A, Onodera O, Funabashi S, Kaneko R, Matsui Y (1993) A numerical and experimental study of sonic boom generated from high speed train tunnels. Int Conf on Speedup Technology for Railway and Maglev Vehicles, Nov. Yokohama pp 305–310

Wu JHT, Ostrowski PP (1971) Shock attenuation in a perforated duct. In: Stollery JL, Gaydon AG, Wen PR (eds) Shock Tube Research, Proc. 8th Int. Symp. on Shock Tubes. Chapman & Hall 15